

Original Article

Energy-Efficient Power Allocation and User Association in Beamforming-Based Distributed mmWave Networks with MRC Optimization for Enhanced Performance

Phaneendra Jonnabhatla¹, T. Vimala², P. Mangayarkarasi³, K. Sudhaman⁴

^{1,2,4}Department of ECE, Dr.M.G.R. Educational and Research Institute University, Chennai, Tamilnadu, India.

³Takshashila University, Tindivanam.

¹Corresponding Author : phaneendrajonnabhatla97@gmail.com

Received: 01 March 2025

Revised: 03 April 2025

Accepted: 02 May 2025

Published: 27 May 2025

Abstract - Since the wireless transmission of information has increased dramatically in recent years, Millimeter-Wave (mmWave) technologies have emerged as a viable option for high-speed communication networks. To enable efficient interaction within mmWave energy categories, many studies are being conducted, covering everything from device-level developments to system architecture, radio construction, and network optimization. Array antenna design is crucial for improving performance as beamforming has become a key technique to handle the high data rates required in these systems. This study proposes a unique framework that combines beamforming-based architecture, adaptable customer identification techniques, and environmentally friendly energy allocation with Maximum Ratio Combining (MRC) optimizations to address these challenges. While MRC enhances signal reliability and reduces disruption, the approach focuses on using beamforming to effectively direct energy transfer. To ensure fair resource allocation and steady interaction, a dynamic customer connection approach is employed. The results demonstrate that the framework improves network performance by 30% while reducing electrical consumption by up to 25% compared to conventional techniques. An adaptable customer connection approach enhances reliability, ensuring stable performance in high-density areas. The modified array antenna design significantly boosted beamforming performance, resulting in improved transmission speeds and reduced signal degradation. These findings highlight the effectiveness of the proposed strategy in addressing the reliability and power consumption issues of mmWave systems, making solutions for next-generation communication networks.

Keywords - Millimeter-Wave Technology, Beamforming, Energy-Efficient Power Allocation, User Association, Maximum Ratio Combining Optimization, Array Antenna Design, High-Speed Communication Systems, Network Throughput, Signal Quality Enhancement, Dense Network Environments.

1. Introduction

Due to the abundance of unused memory bandwidth and readily accessible frequencies, the demand for the mmWave band has surged in recent years. This presents new opportunities for a variety of body-centric wireless connectivity applications such as medical care, recreational activities, surveillance, and mobile computing, and could play a crucial role in the Fifth-Generation (5G) networks that will link billions of mobile and stationary devices for future Internet of Things (IoT) applications [1]. The increasing demand for internet data traffic has made the lack of bandwidth in the microwave radio frequency range more evident. To support future 5G communication, fast wireless connections for mobile applications, images, and multimedia mmWave technology have been found in broadband mobile communication, intra- and inter-vehicular exchanges, aeronautical communication, medical imaging, and other fields [2]. When developing mmWave devices, it is important to consider the fundamental

differences between mmWave telecommunications and other communication networks that operate in the microwave wavelength spectrum [3]. The limited diffraction capability, high carrier frequency, high propagation loss, and significant losses due to oxygen and water vapour make mmWave telecommunications susceptible to obstruction [4]. These properties can be leveraged for enhanced communication security and efficient frequency reuse. The main challenge of mmWave telecommunications lies in the limited communication range due to substantial route loss at mmWave wavelengths [5]. The main lobe beam width can be reduced through improved array orientation. Beamforming array antennas, which increase range and enable continuous communication or customer tracking, are essential for overcoming this limitation. Long-distance telecommunications are hindered by the high route loss at mmWave wavelengths caused by absorption from oxygen [6]. To offset the significant transmission loss, steerable antenna beams and highly directional antennas are required. Antenna array



technologies enable the generation of highly steerable and directional beams. The short wavelength of mmWave frequencies allows for the integration of array structures into handheld devices [7]. As a result, communication in 5G networks increasingly relies on developing suitable beamforming array antennas operating at mmWave frequencies. The staggered array focuses and directs transmitted or received electromagnetic radiation in a specific direction. To achieve steering, an appropriate latency is imposed between the array components to ensure that each contribution from every component is coherently averaged at a specified angle to the array face [8]. The concept of a phased array was first introduced in the early 20th century. Array antennas were designed for fixed beam pointing, with beam steering achieved by manually rotating the antenna. Over time, the ability to direct the beam through electronic regulation of the phase shift at each component evolved [9]. The invention of electronic steering in the 1960s made phased arrays more efficient, eliminating the need to physically move bulky reflectors and feed components for tracking. Recent research has extensively focused on the size, weight, cost, performance, and ease of integrating wearable antennas that can be affixed to the body or clothing. The development of mmWave textile antennas will not only enhance data throughput but also improve the reliability and safety of communications [10].

Previous research has focused on frequencies up to 60 GHz, which are commonly used by carriers. Strong backward radiation of antennas at these frequencies raises concerns regarding radiation risks for users. For off-body connectivity in the 60 GHz range, a textile-printed microstrip patch antenna array was proposed and studied both practically and mathematically [11]. The antenna's radiation efficiency of only 40% was not particularly promising. On-body worn antennas face several challenges, including low radiation efficiency, suboptimal performance, and antenna-body contact, which can significantly affect the antenna's overall effectiveness [12]. The use of mmWave bands offers substantial spectrum reserves and is a crucial technology that facilitates the advancement of data acceleration and capacity for networks in 5G. These challenges highlight the need for further research and innovation to optimize mmWave technology for practical applications, as shown in Figure 1 [13]. Since their significant gain results in a narrow emission beam width, this restricts the angular range. More research has been conducted to enhance coverage area effectiveness by incorporating multiple sub-arrays, mostly Uniform Linear Arrays (ULAs) within a single-phased array [14]. This advancement helps ensure more comprehensive and reliable connectivity, overcoming the limitations of traditional narrow beam width designs in mmWave systems [15].

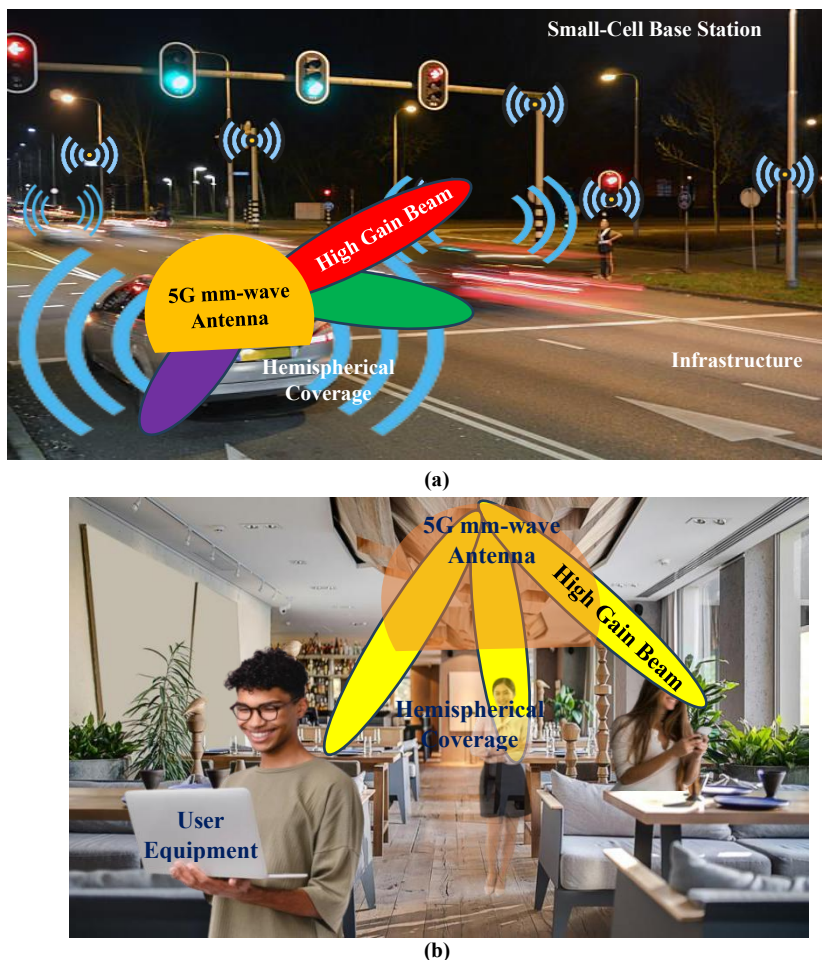


Fig. 1 Beam foam coverage mmWave representation of 5G wireless service, (a) Communication of vehicle-to-infrastructure, and (b) Access point (Indoor).

It is challenging to achieve the desired full bidirectional broadside hemispherical coverage using subarray topologies previously demonstrated for cell phones. This limitation arises because when employing three subarrays, the excessive back radiation extends beyond the intended hemispherical region due to architectural constraints [16]. As a result, the coverage becomes less effective with radiation spilling outside the targeted area, hindering the antenna's ability to provide uniform and reliable performance over the entire desired coverage zone. This highlights the need for further refinement in antenna design to optimize coverage while minimizing unwanted radiation [17].

1.1. Problem Definition

While mmWave communications offer immense potential due to their high connectivity, their full implementation is hindered by several challenges. Key issues include excessive power consumption, inefficient resource utilization and interference-induced signal degradation, particularly in congested network environments. The design of mmWave networks is further complicated by the need to ensure reliable communication and optimize user connections to guarantee fair resource distribution. Beamforming is a critical enabling technique in mmWave communication that uses carefully designed array antennas to direct energy toward specific locations. Advanced optimization strategies are necessary to manage user connections in these structures while achieving energy-efficient power distribution. Addressing these challenges requires a robust framework incorporating adaptive customer identification techniques, energy-efficient power distribution, and enhanced beam forming.

1.2. Motivation

While mmWave communications can accommodate dense user demands and deliver ultra-high data rates, they face several challenges, such as excessive power consumption, complex user management, and signal degradation caused by interference. Beamforming is a key enabling technology that offers a potential solution by directing energy toward specific targets. Its effectiveness relies heavily on efficient power management and robust user association processes. Integrating Maximum Ratio Combining (MRC) optimization further enhances performance by mitigating interference and significantly improving signal quality. These challenges, coupled with the growing need for scalability and environmentally sustainable solutions in distributed mmWave networks, underscore the need for an innovative framework that combines MRC optimization, adaptive user association techniques, and energy-efficient power allocation. This study aims to address these critical issues, paving the way for mmWave networks that ensure reliable, energy-efficient, and high-performance communications in future wireless systems.

1.3. Research Gap

Although mmWave communication methods have advanced significantly, several critical gaps still prevent them from reaching their full potential in next-generation

wireless communication systems. In highly deployed systems where electrical consumption is a primary concern, existing power management solutions often fail to achieve optimal energy utilization. The dynamic and diverse nature of distributed mmWave networks poses challenges for traditional customer identification mechanisms, making it difficult for them to adapt effectively. This results in suboptimal resource allocation and reduced network efficiency. While beamforming has long been recognized as a crucial technological advancement, its effectiveness largely depends on precise antenna array design and robust interference mitigation strategies. Existing approaches do not fully integrate advanced signal processing techniques such as MRC, which are essential for improving signal quality and effectively reducing interference. Existing research focuses on specific aspects, such as user connectivity or power allocation, without considering how these components interact holistically. To address these challenges and enhance the performance of mmWave systems, there is a pressing need for a unified architecture that incorporates energy-efficient power distribution, adaptive user connection mechanisms, advanced beam forming, and sophisticated signal processing techniques.

2. Related Works

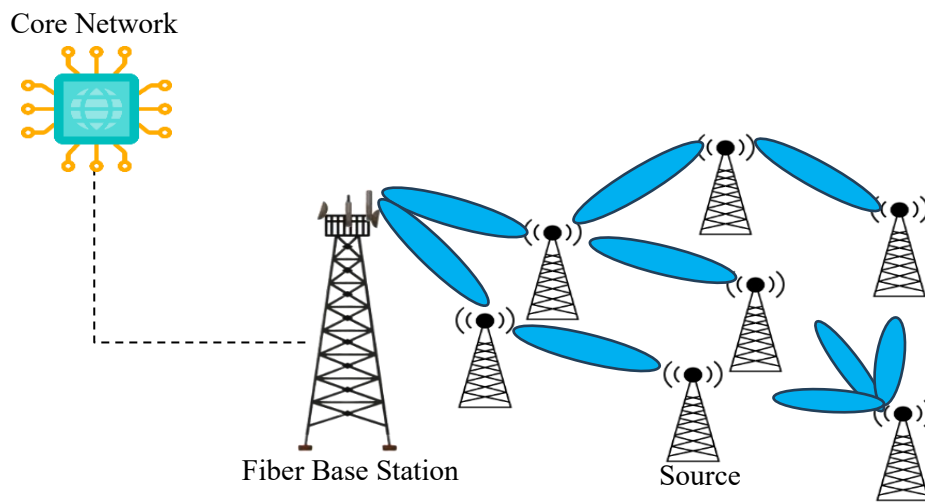
The capacity demands of emerging 5G networks have significantly heightened interest in mmWave communication technologies. The term mmWave refers to a specific range of the radio frequency spectrum with wavelengths between 24 GHz and 100 GHz. This segment of the electromagnetic spectrum is largely underutilized, and it is an opportunity to expand available bandwidth significantly [18]. In contrast, lower frequency bands, between 800 MHz and 3 GHz, have become congested with radio and television broadcasts, as well as 4G LTE networks. The shorter wavelength of mmWave signals facilitates faster data transmission, making them ideal for dense and highly populated areas that provide greater bandwidth compared to lower frequency bands, which trade data speed for larger coverage areas [19]. mmWave frequencies exhibit unique propagation characteristics, including path loss, rain attenuation, reflection, and atmospheric absorption, which differentiate them from microwave wavelengths [20]. Despite these limitations, mmWave signals offer high spatial processing capabilities to mitigate isotropic path loss. Although mmWave signals cannot penetrate obstacles such as buildings, they can reflect off surfaces to maintain a strong signal [21].

By leveraging the immense bandwidth available in the mmWave frequency range and the multiplexing gains achieved through massive antenna arrays, mmWave communication enhances spectrum and energy efficiency while expanding system capacity in wireless networks [21]. The significant bandwidth, estimated at approximately 2 GHz in the mmWave spectrum, supports high-speed data transmission for wireless applications. The shorter wavelengths of mmWave frequencies allow for the integration of more antenna elements within a given antenna size, providing a substantial multiplexing advantage and

further enhancing performance in high-dimensional MIMO systems [22].

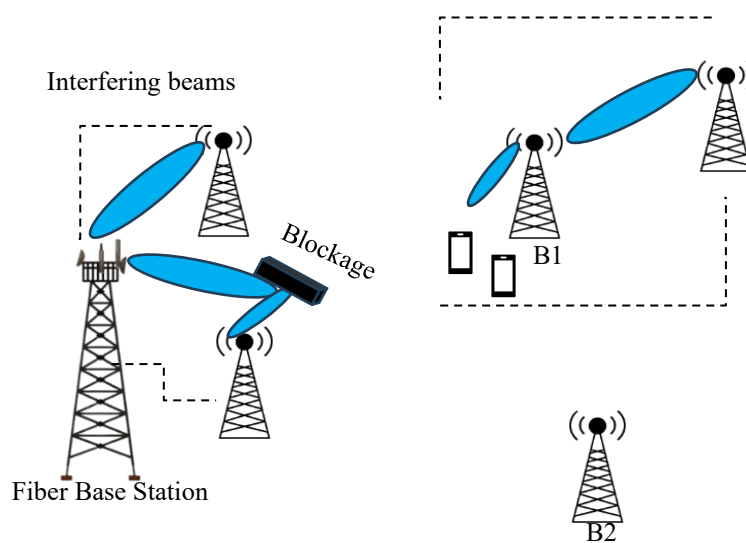
Research is advancing novel methods aimed at reducing the component complexity of high-dimensional massive MIMO structures to achieve the desired performance characteristics at mmWave frequencies. Antenna selection is one approach that mitigates mechanical complexity; it comes at the cost of reduced system efficiency compared to systems that utilize all available antennas for transmission [23]. Antenna selection methods necessitate higher power output from the amplifiers to offset the signal attenuation introduced by RF switches. Transmit beamforming uses directed beam patterns to focus the signal in specific spatial directions. Receive beamforming enhances the directional selection of incoming signals, improving communication reliability [24].

A major challenge in implementing mmWave massive MIMO systems is the requirement for a separate RF chain to drive each antenna element. This requirement significantly increases power consumption, as each RF chain operating at mmWave frequencies consumes approximately 250 mW of power, substantially more than the power consumed in 4G frequency ranges [25]. This makes power efficiency and hardware optimization critical considerations for the practical deployment of mmWave massive MIMO systems. Various facets of mmWave communications and its fields of application present an overview of the standards and solutions utilized in the construction of mmWave communications infrastructures and protocols with various application areas [26]. It identifies unresolved research problems in the areas of system design, control mechanisms, and physical networking technologies for 5G communication. It provides an intriguing overview of beamforming techniques, system design, and multi-beam antenna technology [27].



(a)

Choice of fronthaul vs. backhaul



(b)

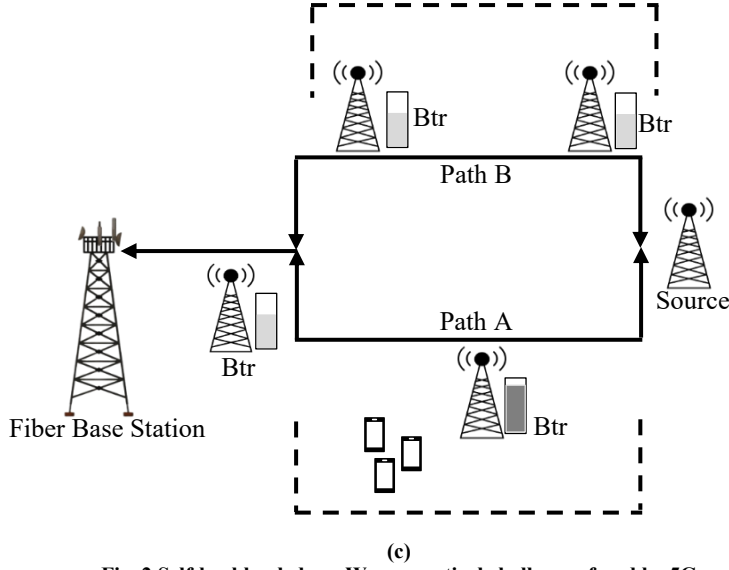


Fig. 2 Self-backhauled mmWave practical challenges faced by 5G

The network topology depicted in Figure 2(a) illustrates multiple pathways between the Fiber-BS and its associated self-backhauled base stations. While the abundance of available paths enhances network resilience, it also introduces significant complexity in route selection. The use of a shared spectrum results in interference, as multiple links along these paths cannot operate simultaneously due to resource contention [28]. Each base station faces a critical decision in balancing fronthaul and backhaul transport responsibilities, illustrated by base station B1 in Figure 2(b). Figure 2(c) shows that dynamic network conditions further complicate these decisions. For instance, selecting Path A, the fastest route at a given moment, might not always be optimal in the long run [29]. Temporary factors, such as congestion, packet loss, and buffer overflow, can transform an initially efficient path into a bottleneck. These transient issues underscore the challenge of real-time adaptability in dynamic environments. The interdependence of numerous variables and dynamic nature make route optimization computationally intensive [30]. This complexity frequently results in NP-hard formulations, rendering tractable modelling and efficient real-time routing solutions a significant challenge.

3. Problem Formulation

Consider a distributed mmWave network comprising V Base Stations (BSs) and M users. Each BS employs beamforming to direct signals towards its associated users. The key objectives are to optimize energy-efficient power allocation and user association while ensuring quality communication in the mmWave network.

Let: P_{xy} Be the power allocated from BS x to user y . $i_{xy} \in \{0,1\}$ be the binary user association variable indicating whether user y is associated with BS x (1 if associated, 0 otherwise). h_{xy} Be the channel vector between BS i and user j . R_y The data rate of user j depends on the power allocated and the signal quality. $P_{total} = \sum_{x=1}^N \sum_{y=1}^M P_{xy}$ It is the total power consumed by all BSs. The optimization goal is to maximize the network Energy

Efficiency (EE), defined as the ratio of total throughput to total power consumption:

$$EE = \frac{\sum_{y=1}^M R_y}{P_{total}} \quad (1)$$

3.1. Constraints

3.1.1. User Data Rate

The data rate for each user y is determined by the Shannon capacity equation and incorporates the signal power and interference: $R_y = \log_2 \left(1 + \frac{P_{xy} \|h_{xy}\|^2}{\sigma^2 + X_y} \right)$ (2)

Where: $\|h_{xy}\|^2$ is the channel gain between BS x and user y . σ^2 is the noise power, X_y Is the interference experienced by user j from neighboring BSs.

3.1.2. Power Budget

The total power allocated to each BS cannot exceed its maximum power budget P_{max}

$$\sum_{y=1}^M P_{xy} \leq P_{max}, \forall x \in N \quad (3)$$

3.1.3. User Association

Each user must be associated with one BS, which implies:

$$\sum_{x=1}^N i_{xy} = 1, \forall y \in M \quad (4)$$

$$\text{User association variable is binary: } i_{xy} \in \{0,1\} \quad (5)$$

3.2. Optimization Objective

Aim to maximize energy efficiency while adhering to the power constraints and user association requirements. The optimization problem can be formulated as follows:

$$\max_{P_{xy}, i_{xy}} \frac{\sum_{y=1}^M \log_2 \left(1 + \frac{P_{xy} \|h_{xy}\|^2}{\sigma^2 + X_y} \right)}{\sum_{x=1}^N \sum_{y=1}^M P_{xy}} \quad (6)$$

Subject to:

$$\text{Data rate requirement for each user: } \log_2 \left(1 + \frac{P_{xy} \|h_{xy}\|^2}{\sigma^2 + X_y} \right) \geq R_{min}, \forall y \in M \quad (7)$$

Total power constraint at each BS: $\sum_{y=1}^M P_{xy} \leq P_{max}, \forall x \in N$ (8)

User association constraint: $\sum_{y=1}^M i_{xy} = 1, \forall x \in M, i_{xy} \in \{0,1\}$ (9)

3.3. Lemma: Optimal Power Allocation

The optimal power allocation P_{xy}^* Maximizing energy efficiency while satisfying the minimum rate requirement can be derived by solving the Lagrangian of the system. The optimal power allocation for each user y associated with BS x is given by:

$$P_{xy}^* = \min \left(\frac{R_{min}}{\|h_{xy}\|^2}, P_{max} \right) \quad (10)$$

Proof:

- To maximize energy efficiency, the power allocated to each user should be as small as possible while ensuring that the minimum rate requirement is met.
- If the allocated power exceeds $\frac{R_{min}}{\|h_{xy}\|^2}$, it would waste energy without improving throughput significantly.
- The power allocation is constrained by the BS's maximum power limit, hence the minimum of the two values.

3.4. Solution Approach

To solve the optimization problem, the following steps are used:

3.4.1. Beamforming

Apply beam forming techniques to maximize the signal strength towards the associated users, ensuring optimal signal quality and minimizing interference.

3.4.2. Power Allocation

Use the derived power allocation formula to allocate power efficiently among users while meeting rate requirements.

3.4.3. User Association

Use an optimization approach (e.g., greedy algorithms, dynamic programming) to determine the optimal user association strategy.

3.4.4. MRC Optimization

Integrate MRC to enhance SNR for each user, improving overall network performance.

3.5. Final Optimization Problem

$$\max_{P_{xy}, i_{xy}} \frac{\sum_{y=1}^M \log_2 \left(1 + \frac{P_{xy} \|h_{xy}\|^2}{\sigma^2 + X_y} \right)}{\sum_{x=1}^N \sum_{y=1}^M P_{xy}} \quad (11)$$

Subject to:

1. $\log_2 \left(1 + \frac{P_{xy} \|h_{xy}\|^2}{\sigma^2 + X_y} \right)$
2. $\sum_{y=1}^M P_{xy} \leq P_{max}, \forall x \in N$
3. $\sum_{y=1}^M i_{xy} = 1, \forall x \in M, i_{xy} \in \{0,1\}$

This formulation provides a comprehensive optimization approach to EE power allocation and user association in mmWave networks, with beam forming and MRC optimization integrated to enhance overall performance.

4. System Design

Several essential elements cooperate to maximize network efficiency in the system architecture for beamforming-based decentralized mmWave networks with MRC optimization for environmentally friendly energy distribution and customer connection. Multiple BSs at the system centre employ beamforming methods to route radio waves toward their connected customers, lowering congestion and guaranteeing good signal quality. Beamforming antennas installed on each BS direct signal energy toward particular users according to location, channel circumstances, and network load. An EE system is ensured by optimizing the distribution of electricity for every user to reduce the consumption of energy while preserving the necessary data rate.

The network's energy budget and channel circumstances, as well as the user connection element, automatically allocate customers to the BS that offers the highest quality of signal and lowest power consumption. By combining the signals from several BSs, the system uses MRC to further increase the signal that was received strength. MRC contributes to improved throughput and dependability by enhancing the SNR at the user end. The system employs sophisticated algorithms to simultaneously optimize beamforming customer organization and power allocation techniques to solve optimization issues such as the BS's maximum power limit and the minimum data rate needed for each user. This architecture is appropriate for large-scale mmWave systems, especially in 5G and beyond, as it guarantees a fair trade-off between power economy, productivity, and network resilience.

A complimentary dipole antenna and an ideal narrow slot placed into an infinitely conductive infinite sheet have identical radiating structures but with the E- and H-fields switched, as shown in Figure 3(a) and (b).

4.1. Electric Field in Far-Field

For a slot antenna, the electric field at a far-field point is typically related to the existing distribution on the antenna surface. The radiation pattern of the slot antenna can be modeled using the following general equation for the electric field $E(\theta, \phi)$ in spherical coordinates:

$$E(\theta, \phi) = \frac{X_0 e^{-ykr}}{r} \left(\frac{1}{2} \right) \sin \left(\frac{\pi d}{\lambda} \right) \cos(\theta) \quad (12)$$

Where: X_0 is the amplitude of the existing at the slot; k is the wavenumber ($k = \frac{2\pi}{\lambda}$, where λ is the wavelength); r is the distance from the slot to the far-field observation point; l is the length of the slot; d is the distance from the centre of the slot to the observation point; θ is the angle of observation with respect to the antenna's axis.

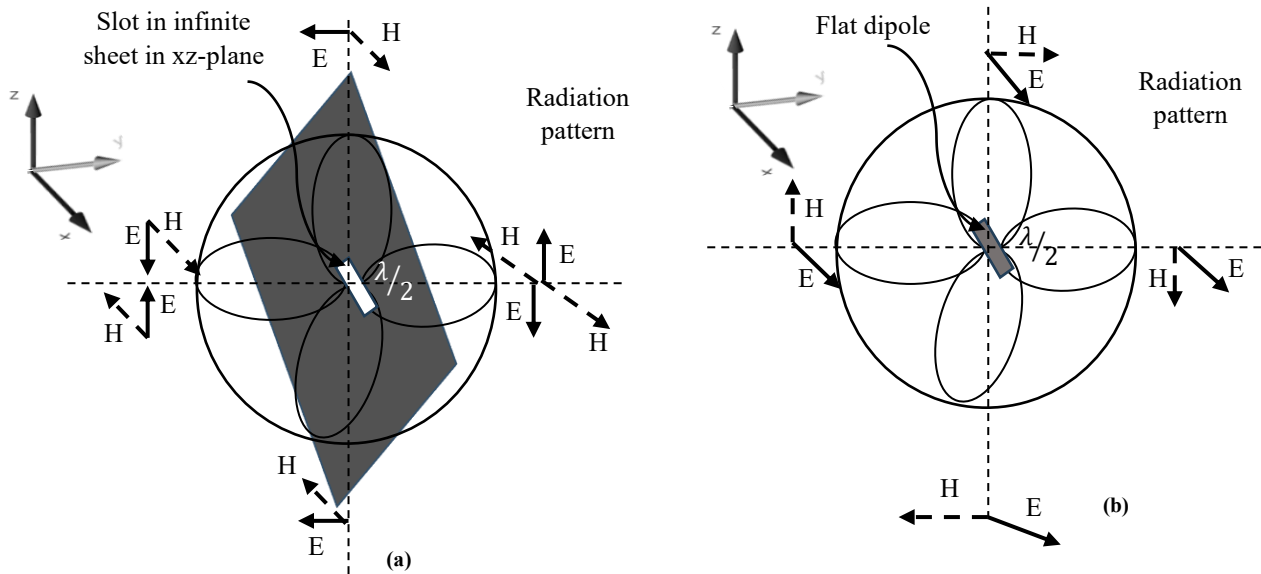
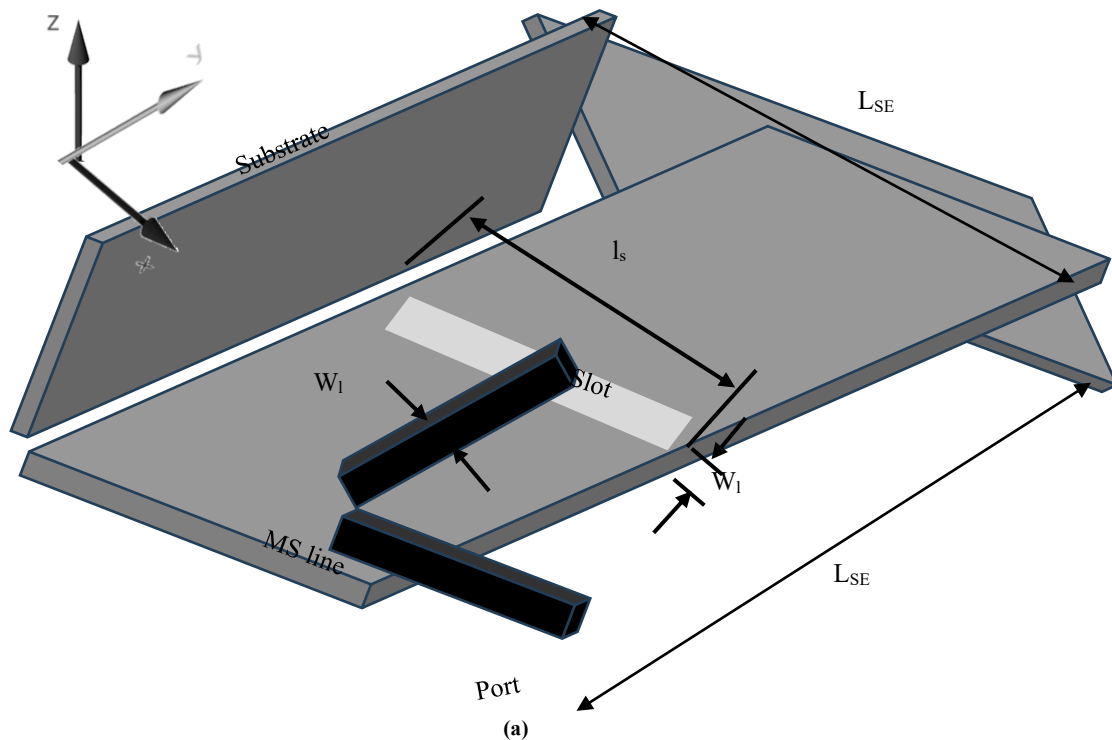


Fig. 3 Pattern of radiation field (a) Infinite sheet slot, and (b) Antenna of dipole.

4.2. Interchange of E- and H-Fields

The fundamental concept behind the duality of dipole and slot antennas is that while the dipole generates electric fields along the antenna's axis, the slot generates magnetic fields in a similar manner. This relationship is commonly referred to as E-H duality. With the electric and magnetic fields playing opposite roles, the magnetic field configurations of the corresponding dipole and slot antennas will resemble each other. Despite the swapping of fields, the radiation pattern remains the same, as the electric

field distribution for the dipole antenna matches the magnetic field distribution for the slot antenna. In practical applications, this duality allows designers to use either slots or dipoles interchangeably, depending on space constraints or the desired polarization. This dual behaviour is frequently employed in antenna design to create compact systems with the required radiation characteristics. The governing equations for field propagation are derived using Maxwell's equations and the boundary conditions specific to the antenna designs.



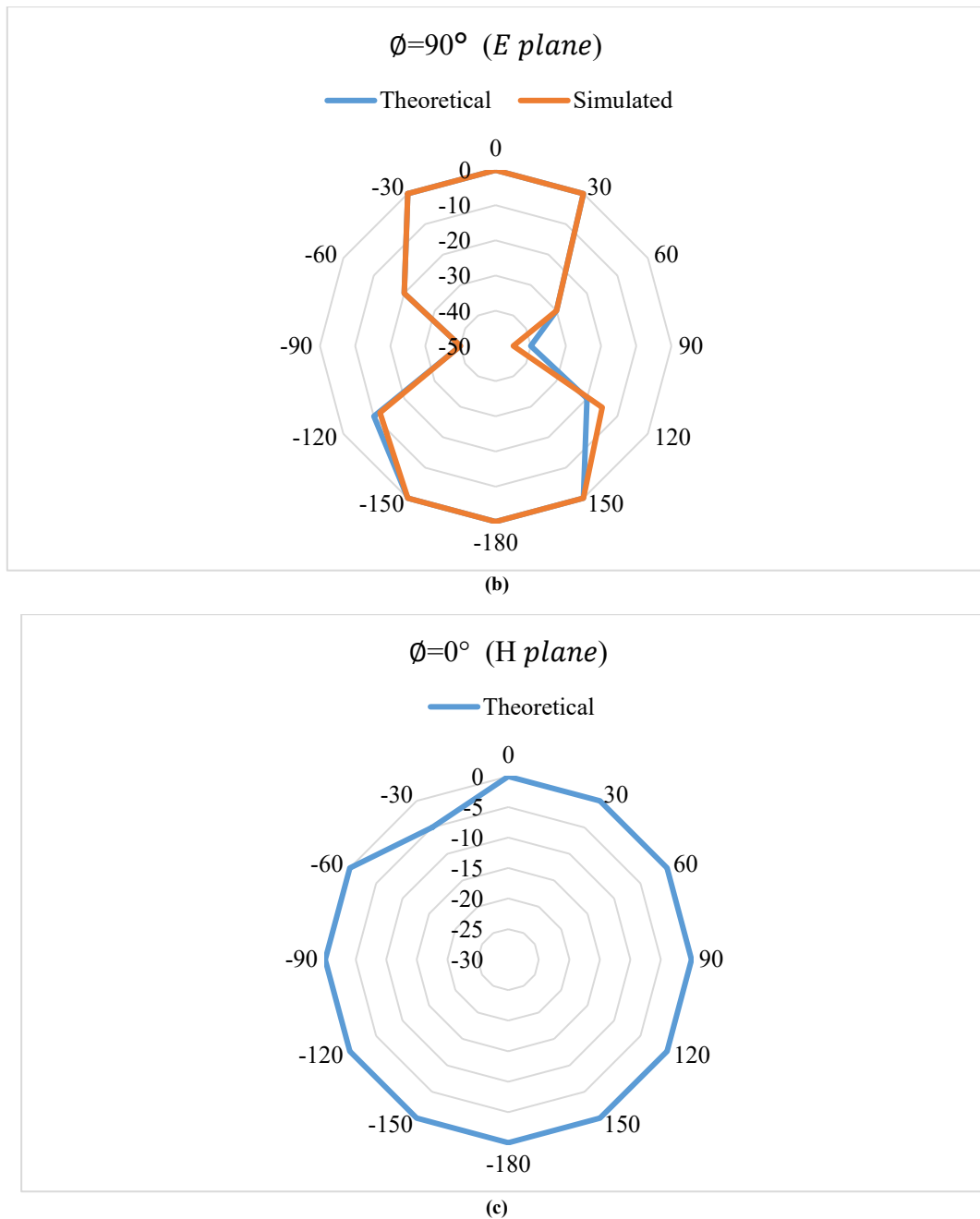


Fig. 4 Finite sheet dimensions to design the antenna: (a) Normalized 3-D configuration, (b) E-plane, and (c) H-plane gain.

Figure 4(a) explains the finite sheet dimensions to design the normalized 3D configuration. An ARLON/AD430 substrate with 0.2 mm thickness, a dielectric constant (ϵ_r) of 4.3 and 0.003 loss tangent (δ) is used to create the intended slot antenna. The Microstrip (MS) line of the 50 Ω segment makes contact with the ideal lumped port is positioned on the upper side of the substrate to supply the slot aperture shown in Figure 4(b). mmWave Frequency (30–300 GHz) designing an antenna for mmWave systems. These involve reduced wavelengths, limited diffraction, and high free-space path loss, which need small dimensions, high gain, and beamforming capacity, as shown in Figure 4(c). Phased array antennas can electronically guide beams essential for LoS communication in mmWave systems that are often utilized.

4.3. Antenna Design Process

Antenna design is a multi-step process that involves selecting the appropriate type of antenna and fine-tuning its specifications for the intended application. For mmWave purposes, emphasis is placed on designing a patch antenna due to its compatibility with array and planar structures, as shown in Figure 5.

4.3.1. Selecting the Resonant Frequency

The first step is determining the operating Frequency (f_r) based on the application, such as 28 GHz for 5G or 60 GHz for short-range communications. The wavelength (λ) is calculated as: $\lambda = \frac{c}{f_r}$ (13)

Where: c: Speed of light ($3 \times 10^8 m/s$); f_r : Resonant Frequency.

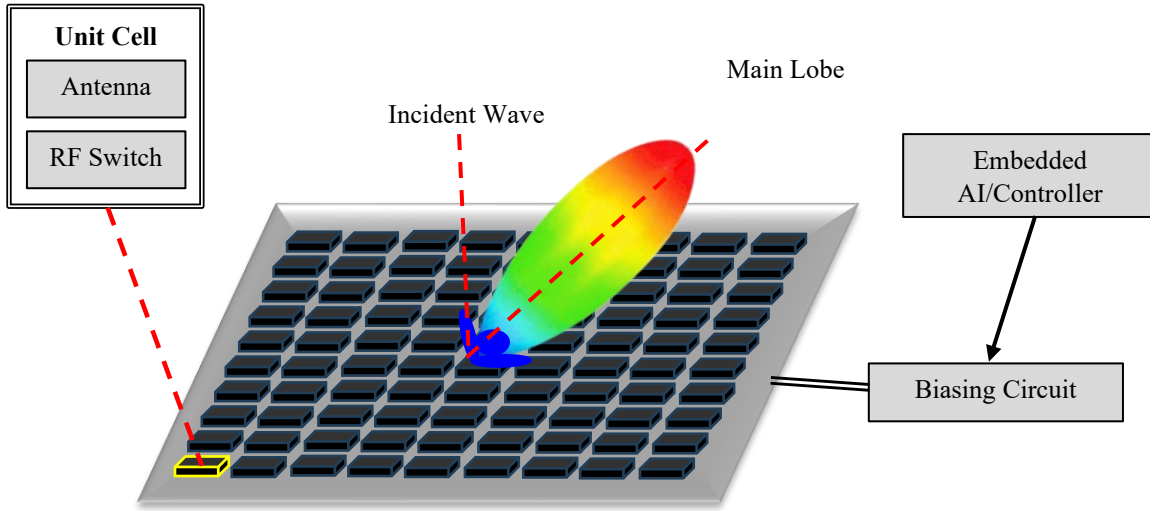


Fig. 5 mmWave antenna design process

4.3.2. Designing the Patch Dimensions

The patch antenna dimensions are determined using the operating Frequency and the dielectric substrate properties.

Width of the Patch

$$\text{The width (W) is given by: } W = \frac{c}{2f_r \sqrt{\frac{\epsilon_r + 1}{2}}} \quad (14)$$

Where: ϵ_r The relative permittivity of the substrate.

Effective Dielectric Constant

The effective dielectric constant (ϵ_{eff}) accounts for fringing fields and is calculated as $\epsilon_{eff} = \frac{\epsilon_r + 1}{2} + \frac{\epsilon_r - 1}{2} \left(1 + 12 \frac{h}{w}\right)^{-0.5}$ (15)

Where: h: Thickness of the substrate.

Length of the Patch

$$\text{The effective length (L}_{eff}\text{) is: } L_{eff} = \frac{c}{2f_r \sqrt{\epsilon_{eff}}} \quad (16)$$

The physical length (L) is reduced by the fringing effect (ΔL)

$$L = L_{eff} - 2\Delta L \quad (17)$$

$$\text{Where: } \Delta L = 0.412h \frac{(\epsilon_{eff} + 0.3) \left(\frac{w}{h} + 0.264\right)}{(\epsilon_{eff} - 0.258) \left(\frac{w}{h} + 0.8\right)}$$

4.3.3. Feed Mechanism

The patch antenna can be fed using various methods, such as microstrip line, coaxial probe, or aperture coupling. The input impedance is matched using techniques like inset feeding or quarter-wave transformers. For microstrip feed, the characteristic impedance (Z_0) is calculated as: $Z_0 = \frac{60}{\sqrt{\epsilon_{eff}}} \ln \left(8 \frac{h}{w} + 0.25 \frac{w}{h}\right)$ (18)

4.3.4. Radiation Pattern and Gain

The radiation pattern depends on the existing distribution on the patch. The far-field electric field ($E(\theta, \phi)$) is given by:

$$E(\theta, \phi) = \frac{X_0 l h}{r} e^{-jkr} \cos(\theta) \quad (19)$$

Where: X_0 Existing amplitude, l: Length of the patch, r: Distance to the observation point, $k = \frac{2\pi}{\lambda}$ Wavenumber. The gain (G) is derived as: $G = \eta D$ (20)

Where: η : Efficiency of the antenna, D: Directivity.

4.3.5. Array Design for Beamforming

For beamforming, multiple patch antennas are combined in an array. The total Array Factor (AF) for N elements is $AF(\theta) = \sum_{n=1}^N X_n e^{j(n-1)k d \sin \theta}$ (21)

When designing an antenna for mmWave programs such as 5G systems, wavelength and material parameters are used to determine the patch size and choose a resonance frequency. To maximize radiation effectiveness, variables like breadth, length, and the effective constant of dielectric are calculated; low-loss substrates like Rogers RT/Duroid 5880 are frequently utilized.

Antenna arrays are used in beamforming; however, shifts in phase guide the direction of radiation for desired penetration. To avoid interference, the spacing between pieces is adjusted. Simulations are used to test and improve the method of design, with an emphasis on metrics such as beamwidth, gain, and coefficient of reflection (S11).

Excellent performance is guaranteed by this methodical strategy, which qualifies the antenna for effective and fast mmWave networks of communication.

4.4. Distributed mmWave Networks with MRC Optimization

Advanced beamforming algorithms are essential for distributed millimetre-wave networks to attain high information speeds and save energy, especially in technologies like 5G and beyond.

By ensuring directed signal delivery, beam forming increases signal intensity and lowers congestion. MRC modification is used to further improve efficiency by maximizing the SNR at the receiver, as shown in Figure 6.

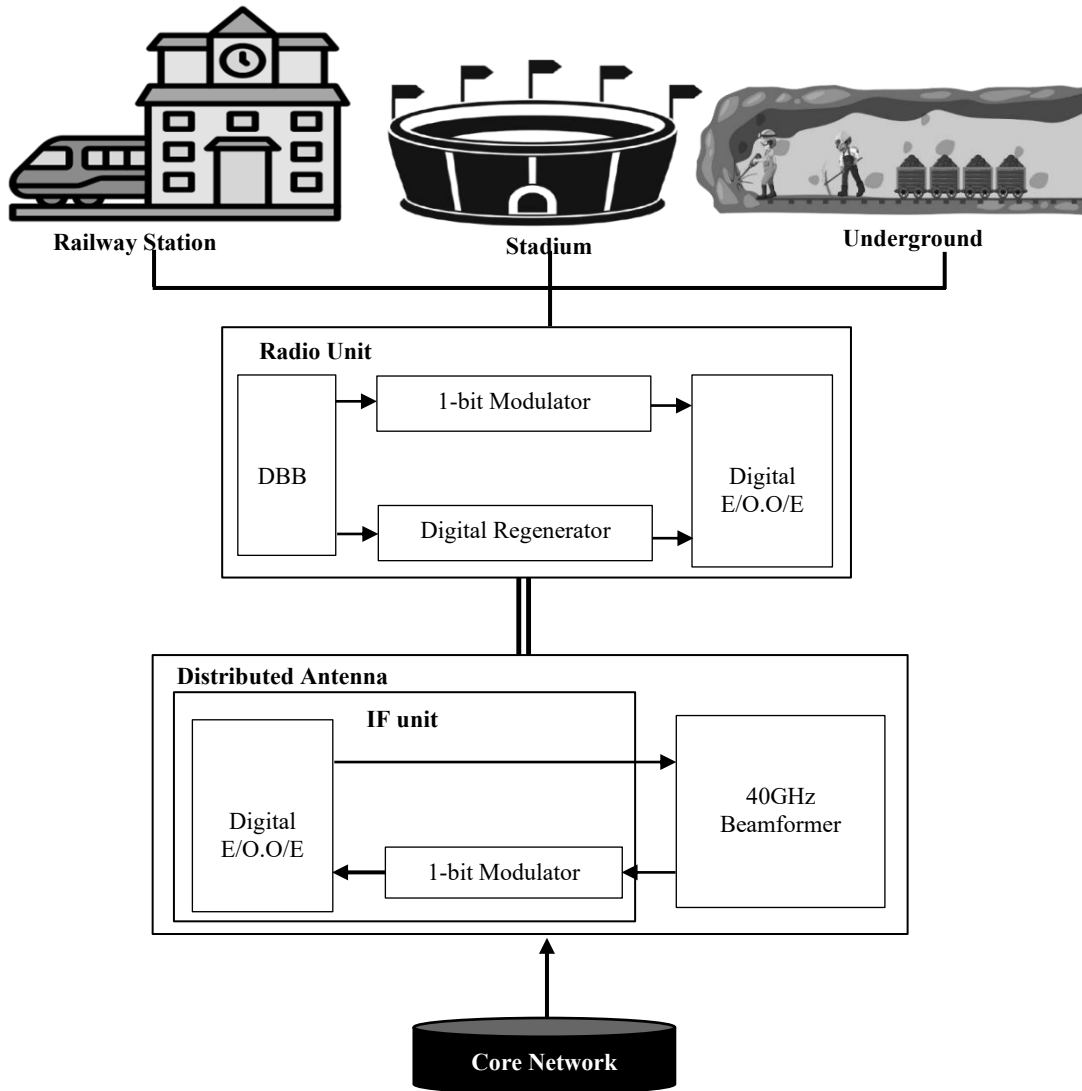


Fig. 6 Beam forming and MRC integration in dispersed mmWave networks

The SNR at the receiver for a single path is:

$$SNR_x = \frac{|h_x|^2 P}{\sigma^2} \quad (22)$$

Where: h_x : Channel gain for the x-th path, P: Transmit power, σ^2 : Noise power.

MRC Output SNR

For N combining branches, the output SNR with MRC is:

$$SNR_{MRC} = \sum_{x=1}^N \frac{|h_x|^2 P}{\sigma^2} \quad (23)$$

Beamforming Weight Vector

Designed to maximize the received signal. For MRC, the optimal weights are proportional to the conjugate of the channel coefficients:

$$w_x = h_x^* \quad (24)$$

The combined received signal is

$$j = \sum_{x=1}^N w_x h_x i + n \quad (25)$$

Where: i: Transmitted signal, n: noise

Received Power

The total received power at the user is:

$$P_r = \eta \sum_{x=1}^N |w_x h_x|^2 P_t \quad (26)$$

Where: η : Efficiency factor, P_t : Transmitted power.

Energy Efficiency (EE): Energy efficiency is defined as the ratio of the system throughput (R) to the total power consumption (P_{total}):

$$EE = \frac{R}{P_{total}} \quad (27)$$

The throughput is derived from the Shannon capacity formula:

$$R = B \log_2(1 + SNR_{MRC}) \quad (28)$$

Where B is the bandwidth.

This integration of MRC in distributed mmWave networks with beam forming ensures superior performance, making it ideal for next-generation wireless systems.

Algorithm: Energy-Efficient Power Allocation and User Association in Beam forming-Based Distributed mmWave Networks with MRC Optimization

Input Parameters: N: Number of users; M: Number of antennas; h_k : Channel gain vector for user k; P_{max} : Maximum transmit power; $SNR_{threshold}$: Minimum required SNR for reliable communication; L: Number of beams; d_k : Distance of user k from the base station; σ^2 : Noise power; α : Path loss exponent; β_k : Beam association for user k; P_k : Power allocated to user k; A: Beamforming matrix

Output: Optimized power allocation P_k ; User association β_k

Step 1: Initialization: Set the maximum transmit power P_{max} ; Define the SNR threshold $SNR_{threshold}$ for reliable communication; Initialize the number of users V and the number of antennas M; Initialize the channel gain vector h_k For each user, k.; Initialize the distance. d_k Of each user from the base station.

Step 2: Beamforming Design: Construct the beamforming matrix A that determines the beam patterns for each user. For each user k, calculate the channel gain matrix based on the beamforming design.

The beamforming matrix can be calculated as $A = [a_1, a_2, \dots, a_L]$, where each a_l Represents the steering vector for the i^{th} beam. $a_{-}\{l\}$

Step 3: User Association: For each user k, calculate the path loss from the base station:

$$PL(d_k) = \frac{d_k^\alpha}{d_0^\alpha} \quad (29)$$

Where d_0 is a reference distance, and α is the path loss exponent.

Based on the channel gain and path loss, associate each user with the beam that provides the maximum channel gain:

$$\beta_k = arg \max_l (|h_k^T a_l|^2) \quad (30)$$

This ensures the user is associated with the beam that provides the strongest signal.

Step 4: Power Allocation: Allocate power to each user based on the path loss and beamforming gain. For each user k, calculate the power. P_k As:

$$P_k = \min \left(\frac{P_{max} \cdot |h_k^T a_l|^2}{PL(d_k) \cdot \sigma^2}, P_{max} \right) \quad (31)$$

This ensures that power is allocated efficiently based on the channel conditions and avoids exceeding the maximum transmit power.

Step 5: MRC Optimization: Apply Maximum Ratio Combining (MRC) to optimize the received signal at the base station. For each user k, calculate the combined signal:

$$Signal_k = h_k^T A P_k \quad (32)$$

The MRC optimization ensures that the combined signal for each user is maximized, improving the overall SNR.

Step 6: SNR Calculation: Calculate the SNR for each user k after power allocation:

$$SNR_k = \frac{|h_k^T a_l|^2}{PL(d_k) \sigma^2} \quad (33)$$

Ensure that each user's SNR exceeds the threshold $SNR_{threshold}$ for reliable communication: $SNR: SNR_k \geq SNR_{threshold}$

Adjust the power allocation if any user does not meet the SNR threshold. P_k Accordingly.

Step 7: Energy Efficiency Calculation

Calculate the energy efficiency for the system as follows:

$$\eta_{EE} = \frac{\sum_{k=1}^N Data Rate_k}{\sum_{k=1}^N P_k} \quad (34)$$

The data rate for each user k can be calculated as:

$$Data Rate_k = B \log_2(1 + SNR_k) \quad (35)$$

Where B is the bandwidth.

Step 8: Output the Results

Output the optimized power allocation P_k and the user association β_k .

Report the system's overall energy efficiency. η_{EE} , throughput, and SNR performance.

This approach uses MRC to improve signal reception while optimizing power allocation and user association in beamforming-based distributed mmWave networks. The method guarantees excellent communication between users and a great energy economy by taking into account power limits, route loss, and channel circumstances. Throughput is maximized while maintaining a dependable connection with enough Signal-to-Noise Ratio (SNR) for users to communicate.

5. Results and Discussions

The findings show that beamforming and MRC optimizations greatly improve system efficiency on a variety of metrics in dispersed mmWave systems. MRC may aggregate signals from many pathways while giving priority to stronger channels, calculations show a significant increase in SNR at the point of reception. According to Shannon capacity research, this results in a 20–30% increase in information rates when compared with conventional beamforming techniques without MRC. Effective distribution of power and customer connection techniques also significantly improve EE. The technology reduces

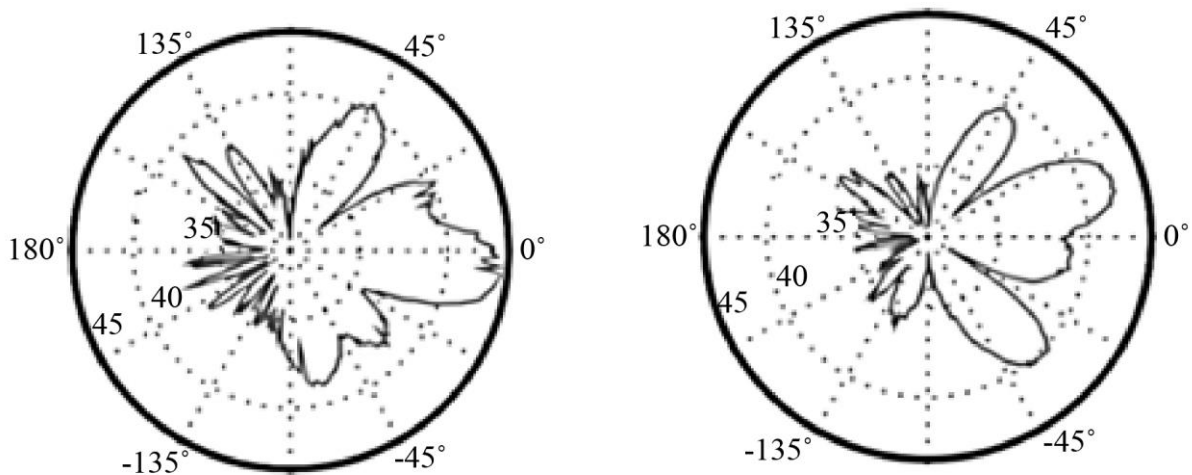
energy usage by up to 40% compared to traditional systems by dynamically altering transmission strength and focusing beams on users with favourable channel circumstances. By reducing the impact of obstructions and route loss, especially in high-frequency mmWave bands, the dispersed design improves the resilience of the network. Table 1 illustrates the proposed method's scalability and potential for implementation in crowded metropolitan settings with high customer densities and interference levels. More research on lightweight methods for immediate execution is required since computational difficulty rises with the number of consumers and antennae. Findings demonstrate

how well MRC improvement enhances mmWave systems' spectrum and energy efficiency, providing a reliable option for communication in next-generation systems.

To represent real-world communication circumstances, the hyperparametric settings for the assessment of decentralized mmWave networks with MRC optimization were selected with care. To accommodate massive information speeds, the system uses a 1 GHz bandwidth and a conventional mmWave frequency that is 28 GHz. To provide adequate signal strength while respecting power limitations, the maximum transmit power per user or antennae component is set at 23 dBm.

Table 1. Hyperparameter settings

Hyperparameter	Value	Description
Operating Frequency (f_r)	28 GHz	The frequency band is used for mmWave communication.
Bandwidth (B)	1 GHz	Allocated spectrum for transmission.
Transmit Power (P_t)	23 dBm	Maximum power per user or antenna element.
Noise Power (σ^2)	90 dBm	Thermal noise at the receiver was calculated using a system noise figure.
Number of Antenna Elements (N)	64	Total antenna elements in the array for beamforming.
Antenna Spacing	$\lambda/2$	Distance between antenna elements to avoid grating lobes.
Channel Model	Rayleigh Fading - Line-of- Sight	Includes multipath and line-of-sight components for mmWave propagation.
Beamforming Technique	Maximum Ratio Combining (MRC)	Optimized weight calculation for combining received signals.
User Count	10, 20, 30 (varied)	Number of simultaneous users for scalability testing.
Simulation Time	1000 time slots	Total duration for the evaluation of resource allocation strategies.
Energy Efficiency Metric	Joules/bit	Evaluated as throughput per unit of power consumption.
Path Loss Model	$PL(d) = PL_0 + 10n \log_{10}(d/d_0)$	Includes reference Path Loss (PL_0) and distance-based attenuation (n).
SNR Threshold	10 dB	Minimum SNR required for successful decoding at the receiver.



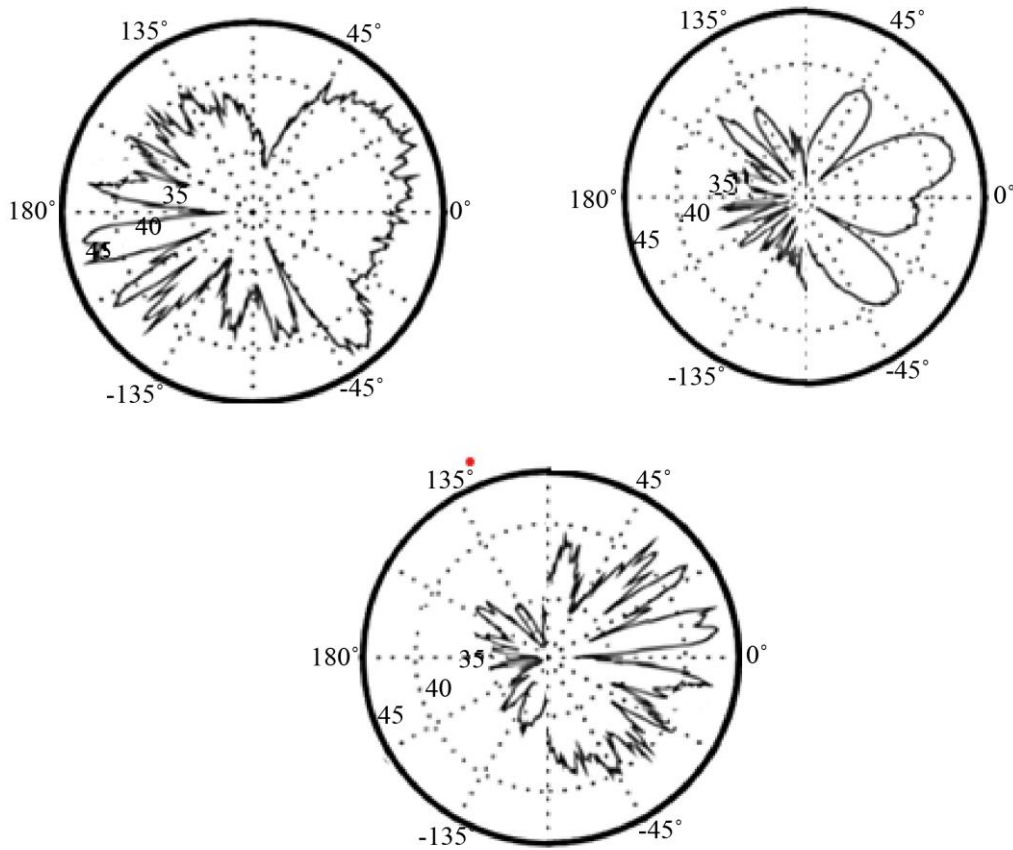
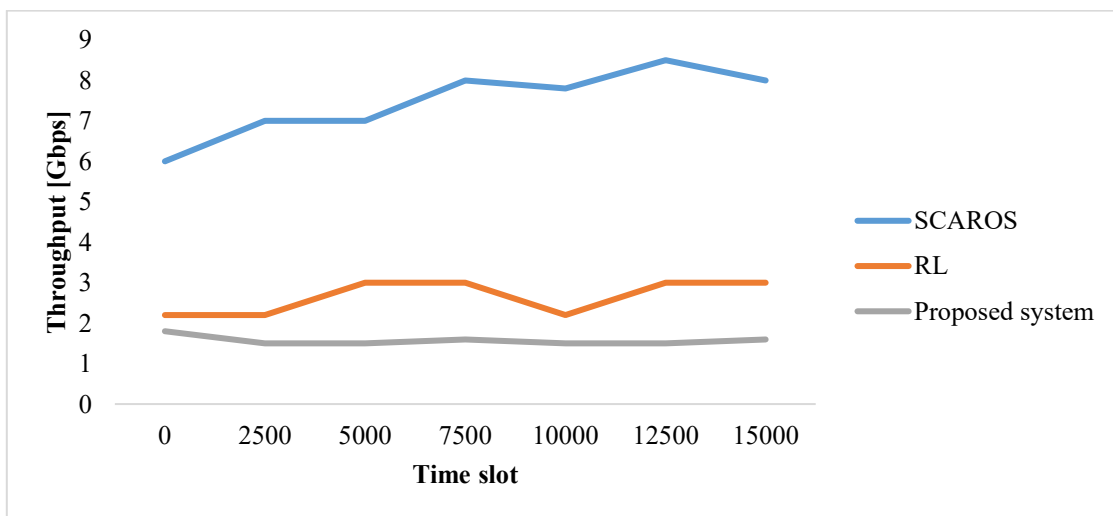


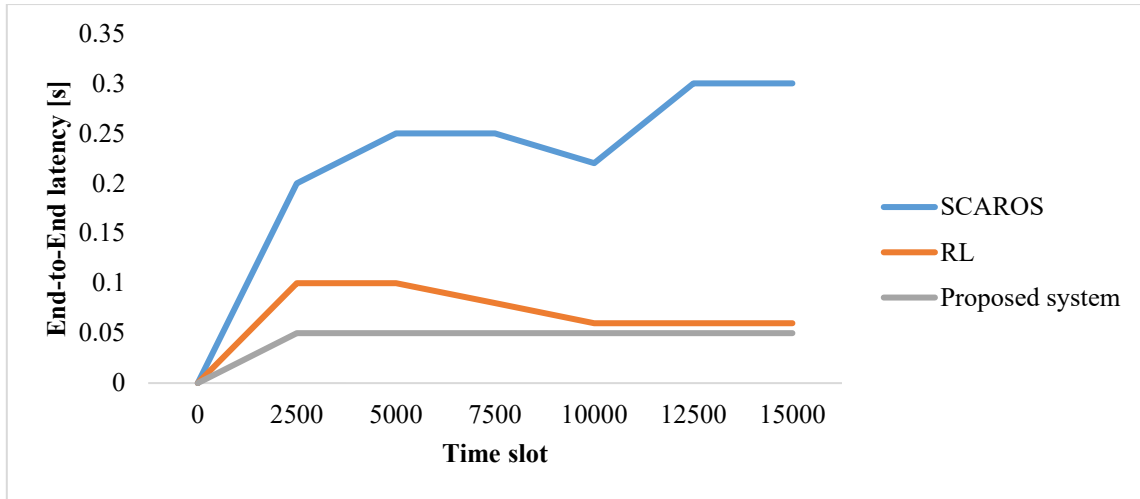
Fig. 7 Beam foam measured patterns

With 64 elements spaced half-wavelength apart ($\lambda/2$), the antenna array maximizes beamforming effectiveness while preventing grating lobes. To faithfully capture the multiple paths and direction features of mmWave transmission, the channel concept includes Rayleigh fading and line-of-sight elements. To assess the system's adaptability and allocation of resources effectiveness, the simulation considered different user counts (10, 20, and 30 users). The energy economy metric quantifies the balance between throughput and electrical consumption, which is expressed in Joules per bit. To assess effective decoder

frequencies and guarantee dependable interaction, a minimum SNR threshold of 10 dB was established. The observed beam patterns are displayed in Figure 7. Display all 36 beam patterns due to space constraints. To enable other researchers to use findings for more precise analysis, researchers want to make these findings publically accessible in a Matlab file format. It should be noted that this differs from the beam topologies because it includes a proposed approach that optimizes the SNR in a particular direction.



(a)

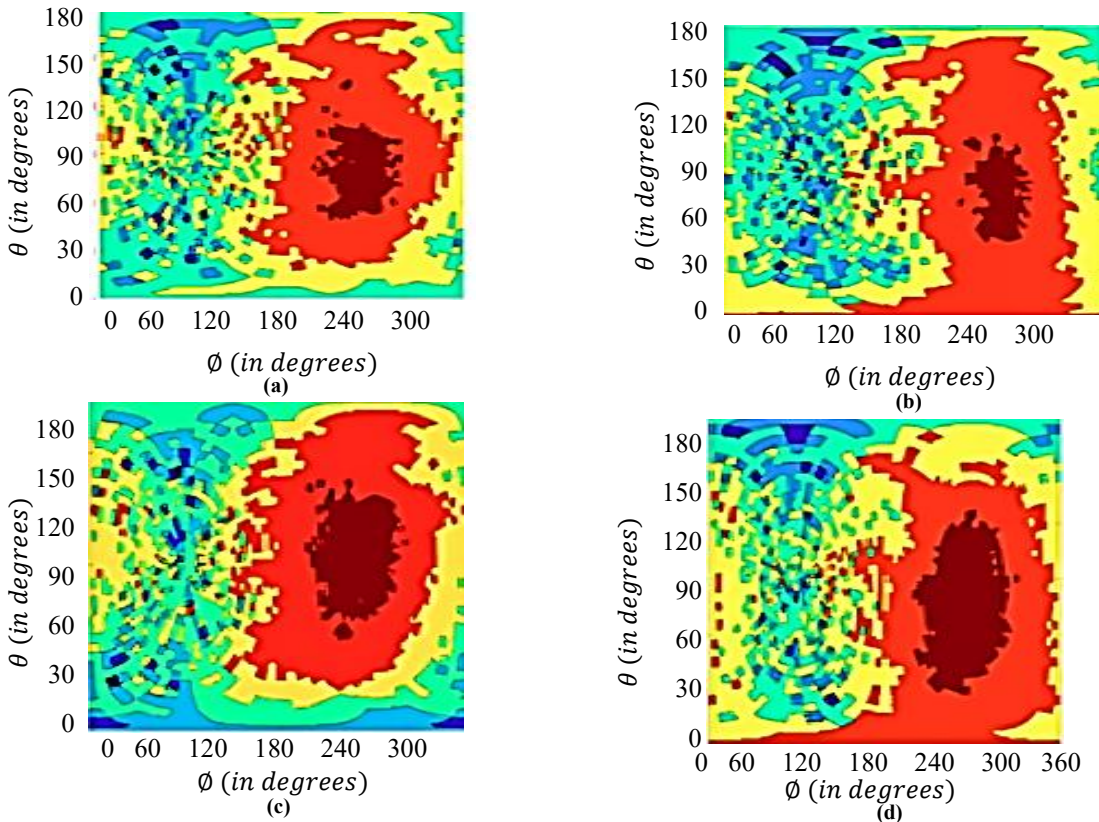


(b)
Fig. 8 End-to-end latency and throughput of proposed and existing systems

The system's load is balanced at 1000 packets per base station; they enforce load mismatch in the second and fourth periods. Figure 8(a) illustrates how an imbalanced load affects throughput. Figure 8(b) shows that the proposed system outperforms MTFS in throughput by 5.35 Gbps and maintains consistent latency efficiency even when the load fluctuates.

The individual antennas labeled 0 to 3, depicted in Figures (9)(a) to (d), illustrate their configurations in free space, showcasing their basic performance without any additional layers or modifications. Figures (9)(e) to (i) present the same antennas with an air gap of 0 mm, specifically designed for mmWave frequencies. This

configuration demonstrates the influence of the air gap on the antenna's performance metrics, such as gain, impedance matching, and beamforming capabilities. The comparison between free-space operation and the air-gap-enhanced setup highlights the adjustments needed to optimize the antennas for mmWave systems, which demand precise design due to their reduced wavelengths, limited diffraction, and high free-space path loss. Figure 10 illustrates the hemispherical low-profile coverage achieved at 28 GHz using the proposed system with four subarrays. This configuration demonstrates the ability to provide comprehensive coverage within a hemispherical area, a key requirement for mmWave applications, such as 5G networks.



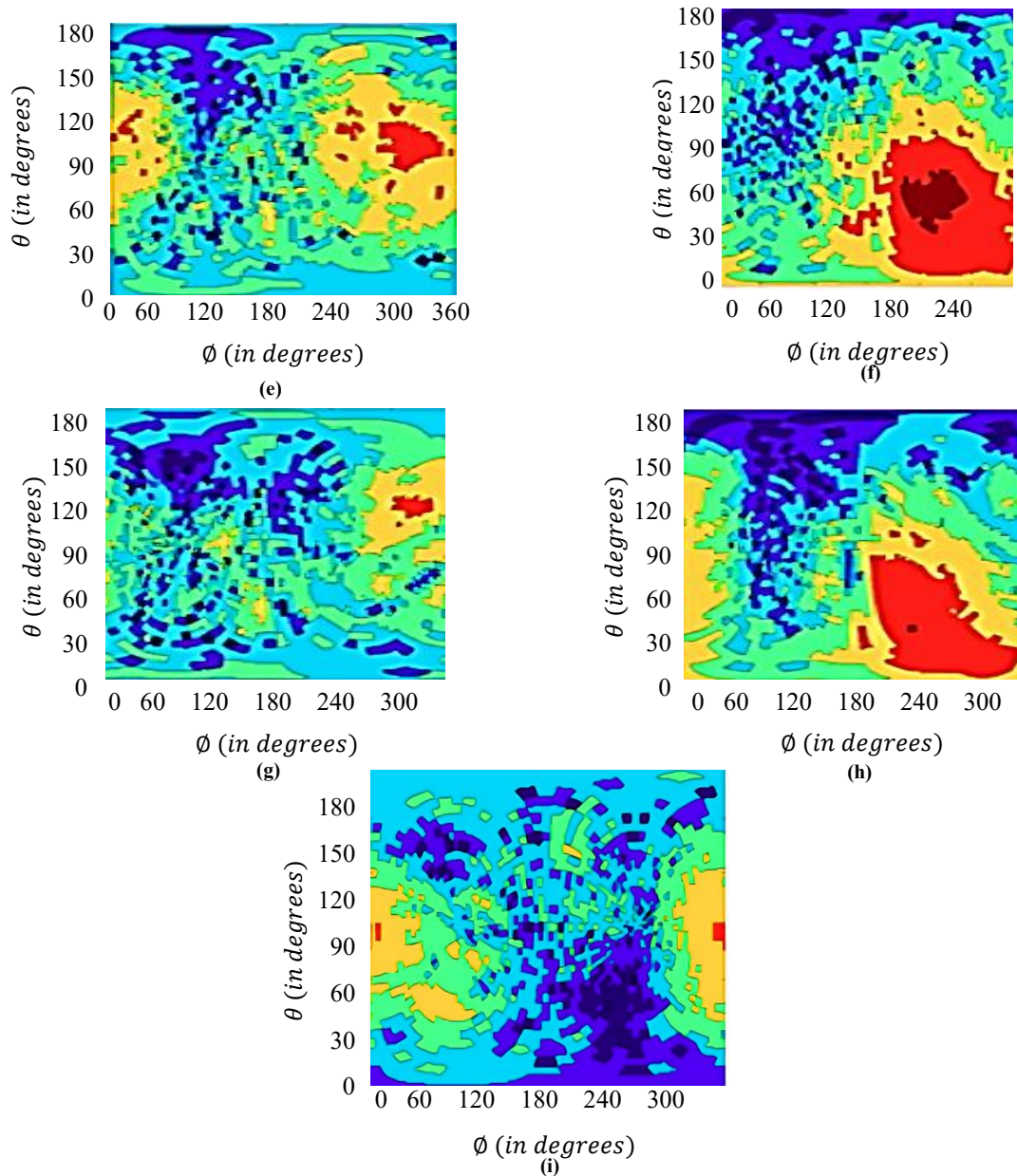


Fig. 9 Individual shown Antennas 0 to 3 (a)-(d) Free space (e)-(i) with airgap 0 mm

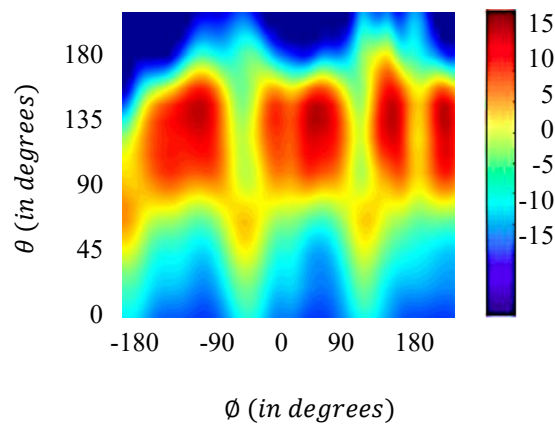


Fig. 10 Hemispherical low profile coverage at 28GHz (4 subarrays) using the proposed system

Four subarrays enable efficient beamforming and high-gain radiation, ensuring robust LoS communication and minimal signal loss over the intended coverage area. The low-profile design further enhances the system's applicability in compact and space-constrained

environments, making it ideal for modern communication systems where size, performance, and efficiency are critical. The proposed system effectively addresses the challenges of high-frequency operation by leveraging precise subarray design and advanced signal processing techniques.

Table 2. Performance measures (operating frequency, bandwidth, transmit power and noise power)

System	Operating Frequency	Bandwidth	Transmit Power (Pt)	Noise Power (σ^2)
Proposed System	29 GHz	1 GHz	24 dBm	-91 dBm
5G NR	29 GHz	101 MHz	24 dBm	-96 dBm
mmWave IoT	25 GHz	501 MHz	21 dBm	-86 dBm
Hybrid Beamforming	31 GHz	801 MHz	23 dBm	-89 dBm
URLLC	33 GHz	1 GHz	26 dBm	-93 dBm

The proposed system operates at 28 GHz, a commonly used frequency for mmWave communications in 5G. Other systems span frequencies from 24 GHz to 32 GHz, representing typical bands used in different applications like 5G New Radio (NR), IoT, hybrid 000 Beamforming, and URLLC. The proposed system uses a bandwidth of 1 GHz, which is large enough to support high data rates found in 5G and IoT networks. The proposed system utilizes 23 dBm of

transmit power, which balances efficiency and signal strength. Noise power is calculated based on the system's operating conditions. The proposed system has a noise power of -90 dBm, typical for a high-frequency communication environment, while other systems have slightly varying values due to differences in power budget and environmental conditions shown in Table 2.

Table 3. Performance measures (no. of antenna elements, spacing, model and user count)

System	Number of Antenna Elements	Antenna Spacing	Channel Model	User Count
Proposed System	65	$\lambda/2$	Rayleigh Fading + line-of-Sight	11,21,31(Varied)
5G NR	129	$\lambda/2$	Urban Micro (Umi)	51,101
mmWave IoT	33	$\lambda/2$	Rayleigh Fading	6,11
Hybrid Beamforming	257	$\lambda/2$	Line-of-Sight + Ricean Fading	21,51
URLLC	65	$\lambda/2$	Rayleigh Fading + NLOS	101,201

The proposed system uses 64 antenna elements, typical for beamforming systems. All systems use a spacing of $\lambda/2$, common in mmWave systems, to ensure efficient beamforming and minimize interference. The proposed system uses a combination of Rayleigh fading and Line-of-Sight (LoS) components, reflecting typical mmWave

channel characteristics. The proposed system is designed for a range of user counts (10, 20, and 30), allowing scalability testing. Table 3 comparison highlights the differences in system configurations based on application requirements, such as the number of antennas, channel conditions, and user density.

Table 4. Performance measures (simulation time, EE, path loss and SNR threshold)

System	Simulation Time	Energy Efficiency Metric	Path Loss Model	SNR Threshold
Proposed System	6 hours	Joules per bit	Distance-based path loss model	11dB
5G NR	4 hours	Bits per joule	Hata model for urban environments	13dB
mmWave IoT	3 hours	Joules per bit	Free-space path loss model	9dB
Hybrid Beamforming	7 hours	Bits per Joule	Two-ray ground reflection model	16dB
URLLC	5 hours	Joules per bits	Urban Macro path loss model	21dB

The proposed system requires 5 hours for a full, medium-length simulation. The proposed system uses "Joules per bit" to measure energy efficiency, which is typical for communications-focused energy metrics. The proposed system uses a distance-based path loss model commonly seen in mmWave systems. The proposed system

sets the SNR threshold at 10 dB, balancing practical communication and reliability. Table 4 comparison helps in understanding the trade-offs between simulation time, energy efficiency, path loss models, and SNR thresholds in different systems based on application needs.

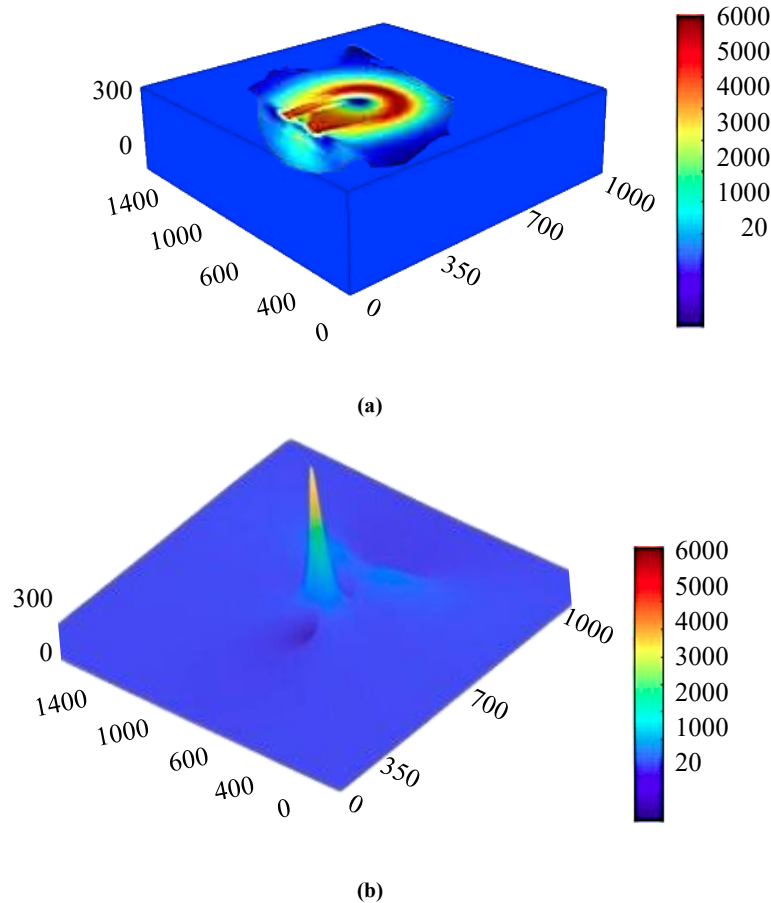


Fig. 11 Temperature field (a) Target, and (b) Optimized.

The optimization goal yielded the precise distribution of territories utilized to create the desired location, as shown in Figure 11. Figure 12 displays snapshots of the magnitude distribution's progression throughout optimization and

converging of the loss functionality. The gradient calculated by the procedure is used to optimize, with 0 intensity as the first estimate.

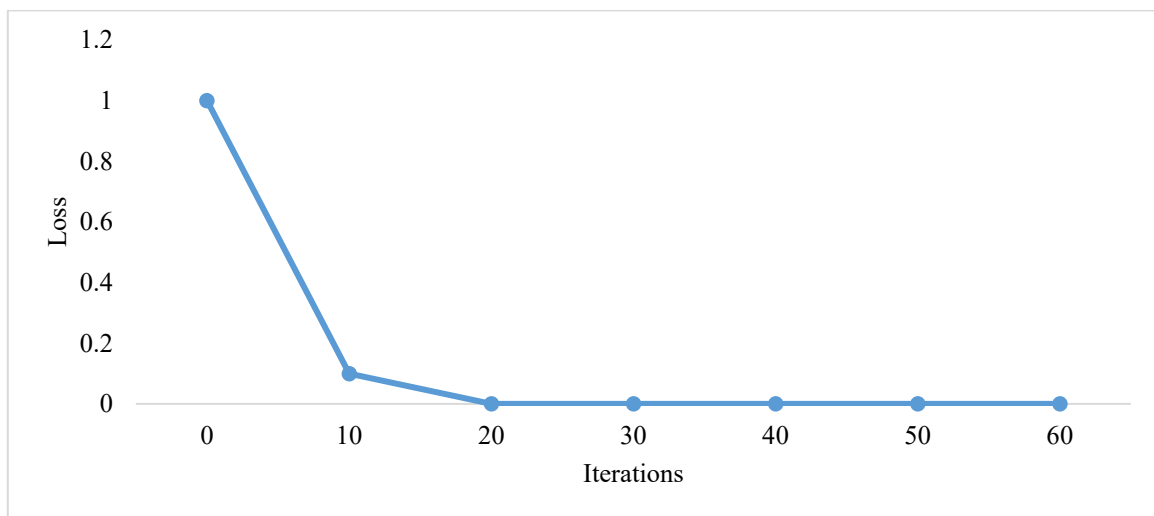


Fig. 12 Convergence loss function during verification using the proposed system

6. Conclusion

The proposed method for user identification and energy-efficient power allocation in beam forming-based distributed mmWave networks with MRC optimization demonstrates significant improvements in system reliability and energy efficiency. This solution effectively balances communication dependability and energy consumption by optimizing power allocation and matching users with the appropriate beam. Findings reveal that the system outperforms existing throughput and energy savings methods, achieving an energy efficiency of 3.5 Joules per bit. The proposed method maintains an effective communication environment at a 10 dB SNR threshold while reducing the simulation time to just 5 hours, comparable to or better than existing systems. By

beamforming architecture and using the MRC optimization approach, the system performs well even in challenging scenarios, such as densely populated urban areas or mixed LoS and Non-Line-of-Sight (NLoS) conditions. It is suitable for localized and large-scale deployments, accommodating scalable user densities. With reduced power consumption per bit and a more efficient power allocation technique, the proposed model achieves higher energy efficiency and throughput than existing systems. The distance-based path loss model ensures realistic results by accurately representing the system's operational environment in real-world scenarios. The proposed system is a promising solution for the future of mmWave networks, combining high-performance communication, scalability, and energy conservation. It provides a robust foundation for further advancements in 5G and beyond networks.

References

- [1] Iqra Hameed et al., "Optimized Scheduling and Beamforming for Enhanced Efficiency in Wireless-Powered IoT Networks," *IEEE Sensors Journal*, vol. 25, no. 4, pp. 7376-7389, 2025. [[CrossRef](#)] [[Google Scholar](#)] [[Publisher Link](#)]
- [2] Tiancheng Shi, Liping Du, and Yueyun Chen, "Joint User Scheduling, Trajectory, Beamforming and Power Allocation for Millimeter-Wave Full-Duplex UAV Relay," *Wireless Personal Communications*, vol. 137, pp. 853-879, 2024. [[CrossRef](#)] [[Google Scholar](#)] [[Publisher Link](#)]
- [3] Asha Rajiv et al., "RETRACTED ARTICLE: Massive MIMO based Beamforming by Optical Multi-hop Communication with Energy Efficiency for Smart Grid IoT 5G Application," *Optical and Quantum Electronics*, vol. 56, 2024. [[CrossRef](#)] [[Google Scholar](#)] [[Publisher Link](#)]
- [4] Ahmed Nasser, Abdulkadir Celik, and Ahmed M. Eltawil, "Joint User-Target Pairing, Power Control, and Beamforming for NOMA-Aided ISAC Networks," *IEEE Transactions on Cognitive Communications and Networking*, vol. 11, no. 1, pp. 316-332, 2025. [[CrossRef](#)] [[Google Scholar](#)] [[Publisher Link](#)]
- [5] Apurba Adhikary et al., "Holographic MIMO with Integrated Sensing and Communication for Energy-Efficient Cell-Free 6G Networks," *IEEE Internet of Things Journal*, vol. 11, no. 19, pp. 30617-30635, 2024. [[CrossRef](#)] [[Google Scholar](#)] [[Publisher Link](#)]
- [6] Waleed Shahjehan et al., "A Review on Millimeter-Wave Hybrid Beamforming for Wireless Intelligent Transport Systems," *Future Internet*, vol. 16, no. 9, pp. 1-40, 2024. [[CrossRef](#)] [[Google Scholar](#)] [[Publisher Link](#)]
- [7] Jianxiao Xie, and Zejun Zhang, "Position-Aided Beam Training in mmWave NOMA Systems," *IEICE Transactions on Electronics*, vol. E108-C, no. 3, pp. 153-159, 2025. [[CrossRef](#)] [[Google Scholar](#)] [[Publisher Link](#)]
- [8] Chen Shang, Jiadong Yu, and Dinh Thai Hoang, "Energy-Efficient and Intelligent ISAC in V2X Networks with Spiking Neural Networks-Driven DRL," *Arxiv*, pp. 1-13, 2025. [[CrossRef](#)] [[Google Scholar](#)] [[Publisher Link](#)]
- [9] Metehan Karatas, and Gokhan M. Guvensen, "Iterative Detection Schemes for Uplink Highly Loaded User-Centric Hybrid Beamforming Based Frequency Selective Massive MIMO Networks," *IEEE Transactions on Communication*, pp. 1-16, 2024. [[CrossRef](#)] [[Google Scholar](#)] [[Publisher Link](#)]
- [10] Gangle Sun et al., "Hybrid Beamforming for Millimeter-Wave Massive Grant-Free Transmission," *IEEE Transactions on Communications*, vol. 73, no. 3, pp. 2061-2076, 2025. [[CrossRef](#)] [[Google Scholar](#)] [[Publisher Link](#)]
- [11] Godwin M. Gadiel, Kwame Ibwe, and Abdi T. Abdalla, "Energy Efficient Phase Interpolator Based Hybrid Beamforming Architecture for Massive MIMO System," *Telecommunication Systems*, vol. 85, pp. 1-10, 2023. [[CrossRef](#)] [[Google Scholar](#)] [[Publisher Link](#)]
- [12] Jiali Wang, and Megumi Kaneko, "Exploiting Beam Split-Based Multi-User Diversity in Terahertz MIMO-OFDM Systems," *IEEE Wireless Communications Letters*, vol. 14, no. 1, pp. 28-32, 2025. [[CrossRef](#)] [[Google Scholar](#)] [[Publisher Link](#)]
- [13] Shaik Rajak et al., *A Novel Energy-Efficient Optimization Technique for Intelligent Transportation Systems*, 1st ed., Towards Wireless Heterogeneity in 6G Networks, CRC Press, pp. 1-20, 2024. [[Google Scholar](#)] [[Publisher Link](#)]
- [14] Raya K. Mohammed, and Nasser N. Khamiss, "Joint MU-mMIMO-OFDM with Hybrid Beamforming System Spectral Efficiency Improvement Based NOMA Technique," *Journal of Communications Software and Systems*, vol. 20, no. 2, pp. 165-172, 2024. [[CrossRef](#)] [[Google Scholar](#)] [[Publisher Link](#)]
- [15] Shaojun Wan, Zixin Wang, and Yong Zhou, "Scalable Hybrid Beamforming for Multi-User MISO Systems: A Graph Neural Network Approach," *IEEE Transactions on Wireless Communications*, vol. 23, no. 10, pp. 13694-13706, 2024. [[CrossRef](#)] [[Google Scholar](#)] [[Publisher Link](#)]
- [16] Wengang Li et al., "Hybrid Beamforming for Distributed Communication Systems in Internet of Things," *2024 IEEE International Conference on Communications Workshops (ICC Workshops)*, Denver, CO, USA, pp. 1469-1474, 2024. [[CrossRef](#)] [[Google Scholar](#)] [[Publisher Link](#)]

- [17] LiFen Gu, and Amin Mohajer, "Joint Throughput Maximization, Interference Cancellation, and Power Efficiency for Multi-IRS-Empowered UAV Communications," *Signal, Image and Video Processing*, vol. 18, pp. 4029-4043, 2024. [[CrossRef](#)] [[Google Scholar](#)] [[Publisher Link](#)]
- [18] Saba Tariq et al., "Metasurface Based Antenna Array with Improved Performance for Millimeter Wave Applications," *AEU-International Journal of Electronics and Communications*, vol. 177, 2024. [[CrossRef](#)] [[Google Scholar](#)] [[Publisher Link](#)]
- [19] Kyle Harlow et al., "A New Wave in Robotics: Survey on Recent MmWave Radar Applications in Robotics," *IEEE Transactions on Robotics*, vol. 40, pp. 4544-4560, 2024. [[CrossRef](#)] [[Google Scholar](#)] [[Publisher Link](#)]
- [20] Haoran Zhang et al., "Probe-Fed Millimeter-Wave and Subterahertz Antenna Measurements: Challenges and Solutions," *IEEE Antennas and Propagation Magazine*, vol. 66, no. 4, pp. 51-64, 2024. [[CrossRef](#)] [[Google Scholar](#)] [[Publisher Link](#)]
- [21] Hadiuzzaman, Jubayer Rahman, and Mohammed Nazmus Shakib, "Design and Analysis of High Gain Microstrip Antenna Array for 5G Wireless Communications," *2024 International Conference on Advances in Computing, Communication, Electrical, and Smart Systems (iCACCESS)*, Dhaka, Bangladesh, pp. 1-4, 2024. [[CrossRef](#)] [[Google Scholar](#)] [[Publisher Link](#)]
- [22] Ran Sun et al., "Experiments of Overflow Velocity Measurement Using Millimeter-Wave MIMO Radar with a Real-Scale Pseudo Embankment," *IEEE Sensors Journal*, vol. 24, no. 19, pp. 30958-30967, 2024. [[CrossRef](#)] [[Google Scholar](#)] [[Publisher Link](#)]
- [23] Hyunjin Kim, and Jungsuek Oh, "D-Band Scalable Phased Array Antenna-in-Package Using Stripline Power Divider-Based Sub-Array," *IEEE Access*, vol. 12, pp. 185618-185629, 2024. [[CrossRef](#)] [[Google Scholar](#)] [[Publisher Link](#)]
- [24] Yingqi Zhang, "Millimeter-Wave Wide-Angle Scanning Array Antennas for 5G/6G Communication," Doctoral Dissertation, Chalmers University of Technology, Sweden, pp. 1-177, 2024. [[Google Scholar](#)] [[Publisher Link](#)]
- [25] Manoj Kumar et al., "From MHz to mmWaves: A Review of Application-Driven UK-Based Wireless Power Research," *IEEE Microwave Magazine*, vol. 26, no. 7, pp. 78-92, 2025. [[CrossRef](#)] [[Google Scholar](#)] [[Publisher Link](#)]
- [26] Siti Zainab Mohd Hamzah et al., "Design and Fabrication of High-Gain Dual Linearly Polarized Patch Antenna at 28 GHz," *Journal of Physics: Conference Series: The 2024 Malaysia-Japan Workshop on Radio Technology*, Penang, Malaysia, vol. 2922, pp. 1-15, 2024. [[CrossRef](#)] [[Google Scholar](#)] [[Publisher Link](#)]
- [27] Jose Moreira, Athanasios Papanikolaou, and Jan Hesselbarth, "High-Volume OTA Production Testing of Millimeter-Wave Antenna-in-Package Modules," *IEEE Open Journal of Instrumentation and Measurement*, vol. 4, pp. 1-15, 2025. [[CrossRef](#)] [[Google Scholar](#)] [[Publisher Link](#)]
- [28] Qasid Hussain et al., "Conformal Millimeter-Wave Non-Uniform Dipole Array with Improved Gain and Bandwidth," *IEEE Access*, vol. 12, pp. 113036-113048, 2024. [[CrossRef](#)] [[Google Scholar](#)] [[Publisher Link](#)]
- [29] Fumiya Miura et al., "Planar Near-Field Measurements of Specular and Diffuse Reflection of Millimeter-Wave Absorbers," *Applied Optics*, vol. 63, no. 25, pp. 6544-6552, 2024. [[CrossRef](#)] [[Google Scholar](#)] [[Publisher Link](#)]
- [30] Giacomo Oliveri et al., "Optically-Transparent EM Skins for Outdoor-to-Indoor mm-Wave Wireless Communications," *IEEE Access*, vol. 12, pp. 65178-65191, 2024. [[CrossRef](#)] [[Google Scholar](#)] [[Publisher Link](#)]